

# Computational modelling of an Organic Rankine Cycle (ORC) waste heat recovery system for an aircraft engine

S. Saadon<sup>1</sup>

<sup>1</sup>*Department of Aerospace Engineering, Faculty of Engineering, University Putra Malaysia, Malaysia*

**Abstract.** Escalating fuel prices and carbon dioxide emission are causing new interest in methods to increase the thrust force of an aircraft engine with limitation of fuel consumption. One viable means is the conversion of exhaust engine waste heat to a more useful form of energy or to be used in the aircraft environmental system. A one-dimensional analysis method has been proposed for the organic Rankine cycle (ORC) waste heat recovery system for turbofan engine in this paper. The paper contains two main parts: validation of the numerical model and a performance prediction of turbofan engine integrated to an ORC system. The cycle is compared with industrial waste heat recovery system from Hangzhou Chinen Steam Turbine Power CO., Ltd. The results show that thrust specific fuel consumption (TSFC) of the turbofan engine reach lowest value at 0.91 lbm/lbf.h for 7000 lbf of thrust force. When the system installation weight is applied, the system results in a 2.0% reduction in fuel burn. Hence implementation of ORC system for waste heat recovery to an aircraft engine can bring a great potential to the aviation industry.

## 1 Introduction

Growing consumption of primary fossil fuels and massive discharge of pollutants are some of the results caused by the world's growing population, and eventually the enlarging energy demand. It is therefore the main concerns that the developing world must face nowadays are the energy shortfall and the environmental destruction. Since 1973, the world energy consumption has been crucially increased and the world energy demands are growing up to 89% starting from 2006 till this year [1]. This affects significantly those industries which waste a huge amount of energy. And for these valid reasons the awareness of the use of the low-grade heat sources has captivated researchers around the world in recent years. To manage this matter, appropriate regulations should be established to further utilize the fossil energy and minimize the misuse energy in a more effective way. Particularly, there is extra effort in the aviation field to reach a higher quality of propulsion system, as the fuel cost is increasing and the future law is becoming more severe. It was recorded that the waste fuel energy from exhaust engine is over 30-40% and only a small fraction of this fuel energy which is roughly 12-25% were converted to useful work [2]. Apart from creating a downturn in fossil fuels market, waste heat recovery will also lead to reduction in greenhouse gases and hence making it the idea of a better future environment more promising.

There are a lot of discussions and researches emerge trying to prove that this waste heat recovery is a practical

resource of energy due to its large quantity [3]. An example of steam-based waste heat recovery system applied to several industries is Heat Recovery Steam Generators (HRSGs). However, it is not recommended for a smaller gas turbine engine due to problems of weight as well as supply of water [4]. Hence an Organic Rankine Cycle (ORC) system has been proven to be one of the beneficial exhaust heat recovery technologies due to its small-scale and its undoubtedly potential integration in the next few years' power supply systems. A Rankine cycle is a heat engine thermodynamic cycle which converts the heat from a device for example turbine into mechanical work. In a Rankine cycle, the system applies the heat to rise up the temperature and pressure of an organic fluid. Thus, the name organic Rankine cycle comes from its use of an organic fluid which has a characteristic of a liquid-vapor phase change at a lower temperature than the phase change in water-steam. This allows heat recuperation of Rankine cycle from a lower temperature. Then this heat recovery can be converted into useful work which can be subsequently transforms into electricity.

Concerning the implementation of the ORC technology, various low-grade waste thermal energy industries such as solar energy, biomass energy, waste heat energy and geothermal energy have considered this system [5]. In power plant applications and marine diesel engine, there have been several researches concerning the thermal analysis and design optimization of an ORC using waste heat source [6-8] and recently a study had also been demonstrated experimentally [9]. Even so, to



To model the evaporator, there are three methods of modelling that can be applied to evaluate the heat transfer of the evaporator. They are distributed modelling, zone modelling and single node lump modelling methods J Sun and W Li [8]. The single node lump modelling approach assumes that the temperature difference inside each node is negligible and this implies that the constant specific heat inside is unchanged too. Hence it is normally not possible for this ORC application where liquid-vapor phase change occurs. Meanwhile, with zone modelling, the evaporator is separated into three different zones which are super-heat, two-phase and sub-cool zones. Consequently, the single node lump method can be applied to each zone. However, a vigorous iterative algorithm is required to attain the heat transfer surface area of each zone. Otherwise, a distributed modelling method treats the evaporator as small divisions starting from where the flow enters until towards the outlet. Then eventually, the single node lump method, here it is NTU (Number of Transfer Units) method, can be applied in each division for evaluation of heat and mass transfers. This distributed modelling method is more accurate compared to the first two methods. In this paper, the distributed method is applied to model the evaporator.

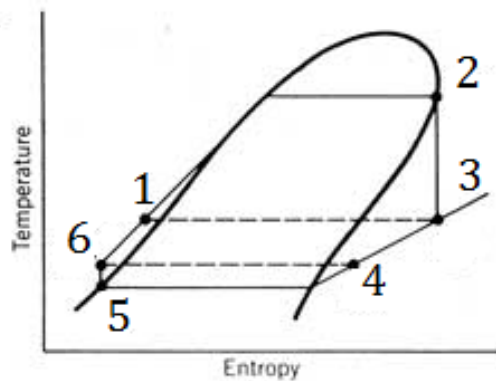


**Figure 2.** T-s diagram of the ORC system with regenerator.

Fig. 3 below shows the three consecutive parts, noted  $i-1$ ,  $i$  and  $i+1$ . By using the distributed modelling method, it is adequate to assume that the heat capacity of the waste heat engine and organic fluid are roughly invariable in each discrete division. Therefore, to construct a numerical model for each single segment, the NTU method is applied. For each segment  $i$ , the enthalpy of the organic fluid is supposed to be increased because the heat is absorbed from the exhaust engine. Consequently, the heat transfer rate of each segment is sum up to get the total heat transfer of the evaporator.

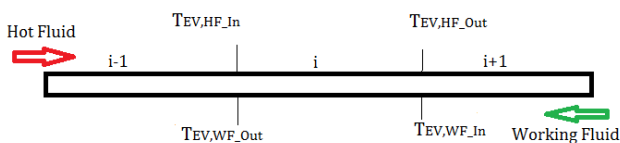


**Figure 3.** Discrete segments of evaporator. [13]

$$q_{EV,Wf}(i) = \dot{m}_{EV,Wf} [h_{EV,Wf\_Out}(i) - h_{EV,Wf\_In}(i)] \quad (1)$$

According to the Eq. 1,  $q_{EV,Wf}(i)$ ,  $\dot{m}_{EV,Wf}$ ,  $h_{EV,Wf\_Out}(i)$  and  $h_{EV,Wf\_In}(i)$  are heat transfer rate, mass flow rate and inlet and outlet enthalpies respectively of the organic fluid for the section  $i$ .

Similarly, the heat transfer rate for the exhaust gas,  $q_{EV,HF}(i)$  is noted as,

$$q_{EV,HF}(i) = \dot{m}_{EV,HF} C_{p,EV,HF}(i) [T_{EV,HF\_In}(i) - T_{EV,HF\_Out}(i)] \quad (2)$$

Here,  $C_{p,EV,HF}(i)$ ,  $\dot{m}_{EV,HF}$ ,  $T_{EV,HF\_In}(i)$  and  $T_{EV,HF\_Out}(i)$  are specific heat, mass flow rate and entrance and exit temperatures respectively of the exhaust gas for the section  $i$ .

The maximum heat transfer rate  $q_{EV,MAX}(i)$ , throughout the evaporator can be written as,

$$q_{EV,MAX}(i) = C_{EV,MIN}(i) [T_{EV,HF\_In}(i) - T_{EV,Wf\_In}(i)] \quad (3)$$

with

$$C_{EV,MIN}(i) = \text{MIN} \left\{ \dot{m}_{EV,Wf} C_{p,EV,Wf}(i), \dot{m}_{EV,HF} C_{p,EV,HF}(i) \right\} \quad (4)$$

Meanwhile, the effectiveness  $\varepsilon_{EV}(i)$  can be defined as [14],

$$\varepsilon_{EV}(i) = \frac{2 \times \left[ \left[ 1 + C_r(i) + (1 + C_r^2(i))^{0.5} \right] \times \frac{1 + \exp \left[ -NTU(i) \times (1 + C_r^2(i))^{0.5} \right]}{1 - \exp \left[ -NTU(i) \times (1 + C_r^2(i))^{0.5} \right]} \right]}{\dots} \quad (5)$$

where  $C_{r,EV}(i) = \frac{C_{EV,MIN}(i)}{C_{EV,MAX}(i)} \quad (6)$

$$C_{EV,MAX}(i) = \text{MAX} \left\{ \dot{m}_{EV,Wf} C_{p,EV,Wf}(i), \dot{m}_{EV,HF} C_{p,EV,HF}(i) \right\} \quad (7)$$

$NTU(i)$  is computed as,

$$NTU(i) = \frac{U(i)A_{EV}(i)}{C_{EV,MIN}(i)} \quad (8)$$

The total heat transfer rate of the evaporator  $Q_{EV}$ ,

$$Q_{EV} = \sum_{i=1}^{N_{EV}} q_{EV}(i) \quad (9)$$

where  $N_{EV}$  is the total of evaporator segments.

The pump power consumption in process 5 to 6 is defined by

$$W_{pump} = \frac{\dot{m}_{WF} C_{p_{WF}} \left( \Pi^{\frac{\gamma-1}{\gamma}} - 1 \right)}{\eta_{pump}} \quad (10)$$

where  $\Pi = \frac{P_2}{P_1}$ ,  $\eta_{pump}$  is the efficiency of the pump and  $\gamma$  is the specific heat ratio of the organic fluid.

When the organic fluid exits the pump as a saturated or superheated fluid and flows through the turbine, the power is produced and exits from the turbine as low pressure superheat fluid. Then the turbine power output is obtained from,

$$W_{exp} = \dot{m}_{WF} C_{p_{WF}} \eta_{exp} T_{exp\_in} \left( 1 - \Pi^{\frac{1-\gamma}{\gamma}} \right) \quad (11)$$

where is  $T_{exp\_in}$  the turbine inlet temperature and  $\eta_{exp}$  is the efficiency of the turbine.

The net power output is then

$$W_{net} = W_{exp} - W_{pump} \quad (12)$$

And the thermal efficiency of the ORC system is

$$\eta_{net} = \frac{W_{exp} - W_{pump}}{Q_{EV}} \quad (13)$$

The total of fuel (kerosene) that could be eventually saved is

$$\dot{m}_{fuel} = \frac{Q_{EV}}{HV_{fuel}} \quad (14)$$

where  $HV_{fuel}$  is the heating value of kerosene,  $HV_{fuel} = 43,000$  kJ/kg.

As the thermal model of the evaporator depends on the effectiveness of the heat exchanger, and this effectiveness itself depends on the  $NTU_{EV}$ , the total heat transfer rate of the evaporator is found numerically by iteration. The procedure is illustrated by the flow chart in Fig. 4. The calculation commences with an initial estimation of  $NTU_{EV}$ . The corresponding organic fluid mass flow rate and heat capacity of both fluids are then calculated, which allows determine the new value of  $NTU_{EV}$  and  $C_{r,EV}$  for each zone. The evaporator effectiveness is then evaluated for each zone. For the first zone, the initial organic fluid mass flow rate is taken as the inlet value. For subsequent zones, the inlet mass flow rate is given by the outlet mass flow rate of the upstream zone. These steps are repeated until the difference between the effectiveness calculated for two consecutive iterations is less than 0.1%. Finally, the heat transfer rate for each zone is calculated and the total heat transfer of the evaporator is attained.

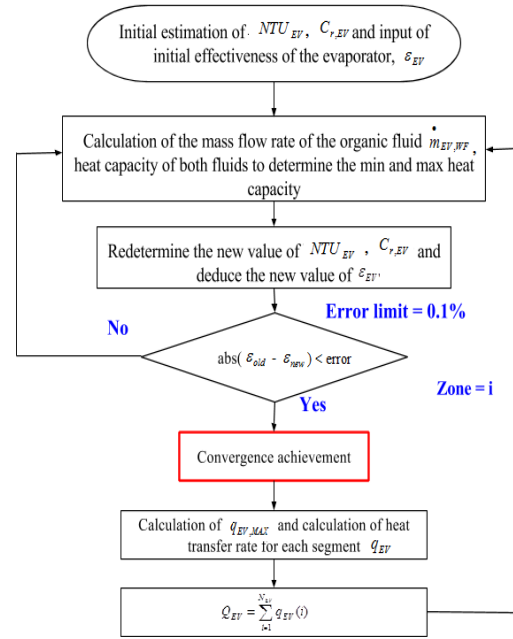


**Figure 4.** Algorithm of calculation of the total heat transfer rate.

### 3 Validation of a thermal model

With the intention to validate the numerical model constructed, the ORC model was first compared to the one for industrial waste heat recovery [15] with R123 at cooling water temperature,  $T_{c,in}$  of 293 K and 303 K. The selected waste heat source is the low temperature steam from Hangzhou Chinen Steam Turbine Power CO., Ltd and is depicted in Table 1 below. The specific heat of R123 in the range of the design temperature value is 0.9744 kJ/kg.K, while for kerosene, it is said to be 2.01 kJ/kg.K. The simulation software is independently developed by the researchers through MATLAB. A simulation is then performed by using the mathematical equations defined above, with inlet temperature of R123 at 100 K.

The model was validated by comparing the results of net power output and system thermal efficiency with the previously published results and these results are presented in Fig. 5 and Fig. 6. It is noted that the net power output and thermal efficiency vary with the inlet temperature heat source. It can be observed that there is a slight deviation compared to the results achieved by Jian Song et al. [15], occurred at higher temperature level of the heat source. These may be resulted from the constant inlet organic fluid assumed in the simulation. Basically, the inlet temperature of R123 will vary with the environmental and factory conditions. The relative error of the results obtained compared to works done by Jian et al. [15] for  $T_{c,in} = 293$  K is 0.43%, while for  $T_{c,in} = 303$  K, the discrepancies is a bit higher at 10.15%. However, for the aircraft engine which the ORC is going to be applied to in the following section, the inlet temperature of the organic fluid used will be given by the engine data and the value is fixed for the design point. As a whole, the numerical solutions obtained in this study are consistent with those reported in Jian Song et al. [15].

**Table 1.** Design parameters of ORC system with R123 as the working fluid.

| Description                   | Unit | Value |
|-------------------------------|------|-------|
| Mass flow rate of R123        | kg/s | 21.2  |
| Heat source inlet temperature | K    | 453   |
| Evaporation temperature       | K    | 350   |
| Turbine inlet pressure        | MPa  | 1.21  |
| Turbine outlet pressure       | MPa  | 0.55  |
| Turbine efficiency            | -    | 0.6   |
| Pump efficiency               | -    | 0.8   |
| Net power output              | kW   | 529   |
| System thermal efficiency     | %    | 12.7  |

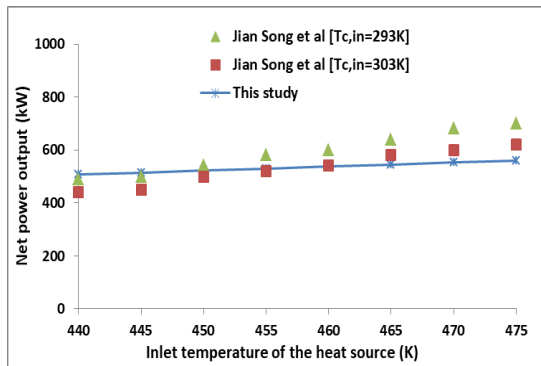


**Figure 5.** Variations of the net power output of the ORC system with heat source inlet temperature.

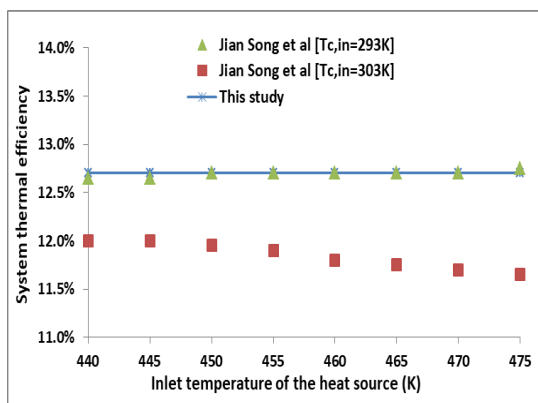


**Figure 6.** Variations of the system thermal efficiencies of the ORC system with heat source inlet temperature.

## 4 ORC integrated to an aircraft exhaust engine

This part presents the advantages of ORC system integrated to a CFM56-7B27 turbofan engine on an aircraft size of 737-800. The working fluid chosen is the R245fa. The specific heat of R245fa in the range of the design temperature value is 1.36 kJ/kg.K. Design parameters are listed in Table 2 below [10]. In order to solve this system, the heat transfer flowing out from the exhaust engine is varied until it matches the heat transfer calculated using the heat transfer coefficient and evaporator area from the detailed design. By doing this, it ensures that the evaporator exit temperature set by the thermodynamic limits of R245fa is maintained. The simulation is then executed as before and the results attained are presented in figure below.

**Table 2.** Main parameter of the ORC system for the turbofan engine

| Description                                   | Unit           | Value |
|---|----------------|-------|
| Mass flow rate of R245fa                      | kg/s           | 3.84  |
| Estimated required surface area of evaporator | m <sup>2</sup> | 23.72 |
| Required heat transfer of evaporator          | kW             | 1105  |
| Exhaust heat temperature                      | K              | 843   |
| Inlet temperature of R245fa                   | K              | 282   |
| Outlet temperature of R245fa                  | K              | 393   |
| Turbine inlet temperature                     | K              | 392   |
| Turbine inlet pressure                        | MPa            | 1.21  |
| Turbine outlet pressure                       | MPa            | 0.55  |
| Turbine efficiency                            | -              | 0.87  |
| Pump efficiency                               | -              | 0.70  |

The turbine within the ORC was connected to a simulation of an external compressor in order to evaluate

the impact on the engine when engine bleed air was reduced. The result shown below in Fig. 7 is detail common cruise conditions with Mach 0.785 at altitude of 35,000 feet. Even with the small loss in core thrust this reduces the TSFC below the base cycle by an average of 3.1%, defined in Fig. 7 by “Regen + Bleed Savings”.

Once the feasibility of the idea of implementing the ORC on an engine basis was confirmed, it was required to estimate the advantages on the combined engine and aircraft system. Fig. 8 described the fuel burn relative to the base cycle and takes into account the vehicle weight throughout the flight. The “Regen + Bleed Savings” scenario show the fuel burn effect only from the TSFC change whereas the “Add 950 lbm per engine” scenario assumes a nominal weight impact of 950 lbm on the detailed ORC system. When the system installation weight is applied, the system results in a 2.0% reduction in fuel burn.

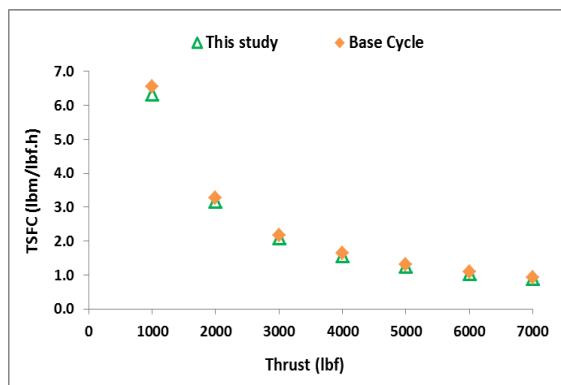


**Figure 7.** ORC engine with TSFC effects and ORC impact on mission fuel burn

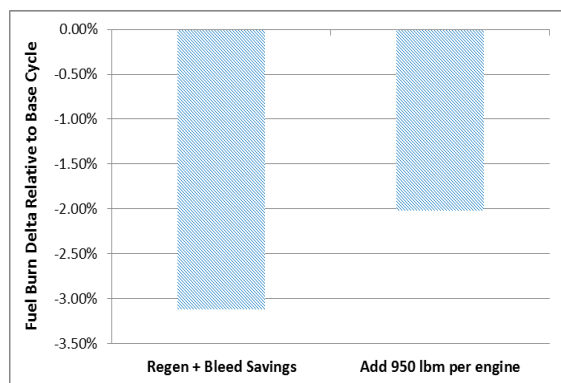


**Figure 8.** ORC engine with TSFC effects and ORC impact on mission fuel burn

## 5 Conclusions

This paper presents a detailed study of a one-dimensional analysis method of ORC system implemented in an aircraft engine. A numerical model for the system has been modified from previous authors’ work. The model features include an algorithm of calculation of the total heat transfer rate driven by the NTU method. Validation with other researchers’ work for an industrial waste heat recovery shows a reasonable agreement with net output

power and thermal efficiency although some discrepancies could be found at higher inlet heat source temperature of the evaporator. These discrepancies can partly be attributed to the assumption of lower organic fluid inlet temperature of the evaporator which results in lower mass flow rate of the fluid. At the same time the simulation model needs more parameters to be defined which increases the variabilities in the simulation estimations.

The initial results for the ORC system integrated to a turbofan’s exhaust engine provide an idea of the impact of this system on the engine’s thrust and its fuel consumption. Parametric optimization shall be conducted in future in order to maximize the total heat transfer rate through the evaporator. Such results will be very useful in future to determine the irreversibility losses through calculation of exergy of each ORC component in order to achieve an optimize system performance and eventually higher thrust power. The presented research proved that an ORC cycle with regenerator gives potential advantages when integrated to an aircraft engine and used to provide electrical power to the aircraft.

## References

1. M. Abdolzadeh, M. Sadeqkhani, A. Ahmadi, *Energy*, **133**, 998-1012, (2017)
2. M. Hasanuzzaman, N.A. Rahim, R. Saidur and S.N. Kazi, *Energy*, **36**, 233-240, (2011)
3. D. Ziviani, A. Beyene, and M. Venturini, *Applied Energy*, **121**, 79-95, (2014)
4. L.Y. Bronicki and D.N. Schochet, *Proceedings ASME Turbo Expo*, **5**, 79-86 (GT2005-68121)
5. B.F. Tchanche, G. Lambrino, A. Frangoudakis and G. Papadakis, *Renewable & Sustainable Energy Reviews*, **15**, 79-95 (2011)
6. J. Song, Y. Song and C.W. Gu, *Energy*, **82**, 976-98, (2015)
7. M.H. Yang and R.H. Yeh, *Applied Energy*, **149**, 1-12, (2015)
8. J. Sun and W. Li, *Applied Thermal Energy*, **31**, 2032-2041, (2011)
9. W. Pu, C. Yue, D. Han, W. He, X. Liu, Q. Zhang and Y. Chen, *Applied Thermal Engineering*, **94**, 221-227, (2016)
10. C.A. Perullo, D.N. Mavris and E. Fonseca, *Proceedings of ASME Turbo Expo. Turbine Technical Conference and Exposition*, (2013)
11. M. Kirby and D. Mavris, *26<sup>th</sup> International Congress of the Aeronautical Sciences*, (2008)
12. J. Schutte, J. Tai and D. Mavris, *48<sup>th</sup> AIAA/ASME/SAE/ASEE Joint Propulsion Conference & Exhibition*, (2012)
13. S. Saadon and A.R. Abu Talib, *IOP Conference Series: Materials Science and Engineering*, **152**, Number 1, (2016)
14. J.P. Holman, *Heat Transfer*, sixth ed. McGraw-Hill Book Company, New York, (1986)
15. J. Song, C. Gu and X. Ren, *Energy Conversion and Management*, **112**, 157-165, (2016)